Arrays of 3D Double-Network Hydrogels for the High-Throughput Discovery of Materials with Enhanced Physical and Biological Properties

Arrays of 3D Double-Network Hydrogels for the High-Throughput Discovery of Materials with Enhanced Physical and Biological Properties

Cairnan Duffy[1]‡, Andrea Venturato[1]‡, Anthony Callanan[2], Annamaria Lilienkampf[1], Mark Bradley[1,]*

[1]School of Chemistry, EaStCHEM, University of Edinburgh, Joseph Black Building, West Mains Road, Edinburgh, EH9 3FJ, UK.

[2]Institute of Bioengineering, School of Engineering, University of Edinburgh, Faraday Building, King's Buildings, Edinburgh, EH9 3Jl, UK.

‡These authors contributed equally

*Corresponding author: mark.bradley@ed.ac.uk

Abstract

Synthetic hydrogels are attractive biomaterials due to their similarity to natural tissues and their chemical tunability, which can impart abilities to respond to environmental cues *e.g.* temperature, pH and light. The mechanical properties of hydrogels can be enhanced by the generation of a double-network. Here, we report the development of an array platform that allows the macroscopic synthesis of up to 80 single- and double-network hydrogels on a single microscope slide. This new platform allows for the screening of hydrogels as 3D features in a high-throughput format with the added dimension of significant control over the compressive and tensile properties of the materials, thus widening their potential application. The platform is adaptable to allow different hydrogels to be generated, with the potential ability to tune and alter the first and second network, and represents an exciting tool in material and biomaterial discovery.

1. Introduction

The surface environment has a direct effect on cell function, proliferation, and differentiation as well as effecting the shape and transcriptome, with the typography of adhesion ligands, soluble factors, and mechanical properties of the surface directly influencing cell phenotype and morphology [1,2]. For example, freshly isolated muscle stem cells rapidly lose their 'stemness' when cultured on 'hard surfaces', such as tissue culture plastic (elastic modulus ~3 GPa), with the cells maintaining their phenotype only when grown on surfaces whose mechanical properties are comparable to that of native muscle [3,4]. Consequently, there is a demand for biocompatible materials that can be tailored for elasticity, hardness and porosity therefore providing the necessary physical cues for cellular function.

Hydrogels are soft materials, typically composed of a polymer network incorporating a large amount of water. Hydrogels have been successfully applied in a range of biomedical applications such as microfluidics, contact lenses, drug delivery and tissue engineering. Moreover, their biocompatibility, defined and pathogen-free composition, reproducible synthesis, porosity (note, gels do not have 'true' porosity), and potential for stimuli responsive properties make them attractive biomaterials, whereas tissue-like materials require control over the mechanical properties. For cell-based applications, stiffness is an important property that is readily modified in hydrogels through varying the level of cross-linking [5,6]. Compared to many tissues, which exhibit good mechanical properties (*e.g.* toughness and shock absorbance), most hydrogels lack the required mechanical strength. To address these issues, new platforms are required that can efficiently identify synthetic materials with the wide diversity of chemical composition and mechanical properties demanded by different cell types and tissues.

Double-network hydrogels are composed of a typically highly cross-linked 'first network' gel containing a 'second' interpenetrating polymer network, with the properties of the two networks varying in density, rigidity, molecular weight, and level of cross-linking [7]. This approach has produced hydrogels that are considerably tougher than the corresponding single-network gels, with optimised double-network hydrogels having been generated that are hard (0.1–1 MPa), strong (tensile stress 1–10 MPa, compressive stress 20–60 MPa), tough (tearing fracture energy 100–9000 Jm^{-2}), and which can be stretched up to 20 times their own length [7,8]. The improved toughness and stretchability of these hydrogels has been proposed to be a consequence of the contrasting properties of the two interweaving networks, with the first highly cross-linked network being stiffer but prone to fracture and the second loosely

cross-linked network allowing greater extension and energy dissipation at the point of fracture [7,8]. Double-network hydrogels have been applied as biomaterials with similar properties to cartilage tissue [9] with double-network combinations including poly(2-acrylamido-2-mehtylpropanesulfonic acid), alginate, or poly(ethyleneoxide) (PEO) as the highly cross-linked first network with poly(acrylamide) or poly(acrylic acid) (combined with PEO) as the loosely cross-linked second network [8,10,11].

Polymer microarrays [12,13] have enabled the high-throughput discovery of biomaterials with various properties, including polymers for the isolation of osteoblasts for bone tissue engineering [14], isolation and growth of functional hepatocytes [15] and platelet activation [16]. Other relevant applications include substrates to capture/repel various pathogens [17–20] and substrates for long-term defined stem cell culture [21–24]. However, despite its screening power, this 2D platform is not suitable as such for the screening of hydrogels' mechanical properties and cannot be readily adapted to produce 3D scaffolds.

Here, we report the development of a hydrogel array that allows up to 80 unique 3D features on a single microscope slide. This approach utilised a 3D printed mould, which enabled a production of a mask with 80 'reaction wells' that could be placed over a glass slide. Hydrogel features were photo-polymerised *in situ* in the mask wells followed by mask extraction and the generation of a second polymer network with acrylamide. This allowed the formation of 3D double-network hydrogel features on the array with varying properties such as stiffness and elasticity. Combined with the classical 2D polymer microarray technology, this new 3D platform provides a powerful pipeline for the identification of biomaterials with a wide range of properties and subsequent optimisation of 3D scaffolds for various applications.

2. Materials and Methods

All chemicals were purchased from Sigma-Aldrich unless specified otherwise. Sylgard 184 (PDMS) was purchased from Down Corning, printing filaments from Ultimaker 1, Elastomer kit (Mold Star 15 Slow) from Smooth-On, and glass slides from Thermo Scientific. Cell culture reagents were purchased from Invitrogen unless otherwise stated.

2.1. Preparation of glass slides

A 2% agarose solution was prepared by adding 4 g of agarose l-B (Sigma-Aldrich) to 200 mL of sterile water. The solution was heated until the agarose dissolved and incubated at 70 °C in

a water bath. Glass slides were dip-coated by immersion into the agarose solution and dried at room temperature overnight. The agarose layer on the bottom of the slides was removed with ethanol using tissue paper.

2.2. Mask fabrication

A custom 80-well mould for the 3D masks was designed using Autodesk Inventor software (Fig. 2A) and printed using a customised 3D printer (Ultimaker 1, B.V, The Netherlands) with a 0.4 mm nozzle and commercially available polylactic acid (PLA) filament (2.85 mm diameter, Ultimaker 1, B.V, The Netherlands) (Fig. 2B, left). Customisation of the printer consisted of a 3D printed ventilator fan, four belt-tensors and four platform supports. Moulds were printed with the following parameters: layer height 0.1 mm, shell thickness 0.2 mm, printing temperature 225 °C, print speed 30 mm/s, and filament flow 110%. A PLA raft support platform was printed prior to the mould to provide better adhesion to the surface.

For the mask, the two components of the elastomer kit (Mold Star 15 Slow) were mixed in a 1:1 ratio until a homogeneous mixture was obtained. A glass slide (76 × 26 mm) was applied over the mould (paper tape was used to affix the glass slide to the mould). The cavity of the mould was completely filled with the elastomer (3.2 mL) with a syringe and left to cure for 6 h at room temperature. The PLA mould was removed and the silicon-based mask peeled-off from the glass slide. The silicon film on the bottom of each well on the mask was gently removed using pliers.

2.3. 3D array fabrication

A 1.5 M solutions of 2-(acryloyloxyethyl) trimethylammonium chloride (AEtMA-Cl), *N,N*-diethylacrylamide (DEAA), *N*-isopropylacrylamide (NIPA), *N*-(1,1-dimethyl-3-oxobutyl)acrylamide (DMOBAA), 2-(dimethylamino)ethyl methacrylate (DMAEMA), poly(ethylene glycol) methacrylate (PEG_6MA), 2-carboxyethyl acrylate (CEA), ethylene glycol methacrylate phosphate (EMAP), and *N,N*-dimethylacrylamide (DMAA) in 1-methyl-2-pyrrolidinone (NMP) were prepared. A 1.1 M stock solution (5 mL) of *N,N'*-methylenebisacrylamide (MBA) in NMP was prepared and serial dilutions were performed to allow modification of the MBA concentration while keeping the printing volume constant. All solutions were stored at 4 °C.

The mask containing 80 reaction wells was applied on the agarose coated glass slides (the smooth surface of the mask adheres to agarose). Monomer solutions were dispensed into each reaction well using a bioprinter (PolyPico, Ireland) utilising cartridges with 100 μm aperture (the volume depending on the monomer ratio in the target hydrogel, see Table S2), to give a total volume of 2.6 μL/well. Impulse intensity and impulse width parameters were calibrated for each new cartridge load. Subsequently, 0.65 μL of MBA solution and 0.65 μL 1-hydroxyclyclohexyl phenyl ketone (1 M in NMP) were dispensed, consecutively, using a cartridge with a 100 μm aperture, to give final volume of 3.9 μL/well (total monomer concentration 1M). The array was photo-polymerised for 30 min using CL-1000 ultraviolet cross-linker (UVP Inc.) (385 nm, 1 J/cm^2), after which the silicon mask was peeled off leaving structured hydrogels on the slide surface.

To generate the second network, the arrays with the 'first network' features were placed into 4-well chamber slides and 5 mL of 2 M acrylamide (aq) with 0.1 mol% of MBA and α-ketoglutarate was added per array and the slides were incubated overnight. The excess solution was removed and the slides were polymerised under UV light (385 nm, 1 J/cm^2) for 30 min.

2.4. Preparation of hydrogels for mechanical testing

To generate hydrogels for compression testing, the monomers, cross-linker MBA and 1-hydroxyclyclohexyl phenyl ketone (in NMP) were placed in a PDMS mould cylindrical wells, (diameter 6.33 mm × 2 mm). The mixture was polymerised for 1 h under UV light (385 nm, 1 J/cm^2) using CL-1000 ultraviolet cross-linker (UVP Inc.). The hydrogels were removed from the mould and placed in a vacuum oven at 40 °C overnight. These samples were placed into wells of a 12-well plate. For single-network hydrogels, 1.6 mL of water was added to each well. For double-network gels 1.6 mL of 2 M acrylamide (aq) with 0.1 mol% of MBA and α-ketoglutarate were added and the samples were incubated for 24 h (where the mol% of the cross-linker and the molarity of the second network were changed, the concentrations were adjusted accordingly). The excess second-network solution was removed and the samples were polymerised with UV for 1h (385 nm, 1 J/cm^2), after which 1.6 mL of water was added to each well. The gels were stored at room temperature.

For tensile testing, the components for the first network (see above) were placed in 'dog bone' shaped PDMS mould with a volume of 890 μL and the mixture polymerised for 1h under UV light. The hydrogels were removed from the moulds and transferred into polystyrene

containers (12 × 4 × 2 cm) and submerged in to a solution (20 mL) containing the components for the second-network. After 24h incubation, the excess of the solution was removed and the hydrogels polymerised for 1h under UV light. The double-network hydrogels were stored in water.

2.5 Compression and tensile testing

Single- and double-network hydrogel samples were tested using an Instron Model 3367 using Bluehill 3 software (Norwood, MA, USA), equipped with a 50N load cell for compression and tensile analysis. All sample measurements were taken using a digital vernier callipers and micrometer (0–25 mm range and 0.001 mm accuracy).

The compression tests were performed on cylindrical samples using two different strain rates. Three tests were performed using the two different stain rates. At the 0.5 % min^{-1} strain rate samples were loaded to 10 % strain with stiffness calculated between 5–10 % strain. For the 5 % min^{-1}, samples were compressed to 10 % strain and 60 % strain with stiffness calculated between 5–10 %, and 50–55 % strain, respectively. Stiffness was calculated using the incremental tangent modulus using an extrapolation method as previously described [25].

The tensile testing was performed on 'dog bone' shaped samples based on ISO standards. Single- and double-network hydrogel samples were clamped at each end for lengthwise testing, and tested at a 30 % min^{-1} extension rate until fracture. Failure tensile strength and failure strain were determined from stress-strain curves in which the ultimate tensile strength was taken as the maximum stress.

2.6. Scanning electron microscopy

The arrays were sectioned into 4 parts using a glass cutter (46004TCT, Scriber) and each piece was immersed in liquid nitrogen, placed in cold flask (cooled with dry ice), and lyophilised overnight *in vacuo* (< 1 mbar). The dried samples were gold coated by spluttering. A Phillips XLS30CP scanning electron microscope was used to image the surfaces samples.

2.7. Cell culture

HeLa cells were grown on 25 cm^2 tissue culture flasks (Corning) in DMEM supplemented with 10% FCS (BIOSERA FB-1090/500), L-glut (100 units, Ml Gibco 25030-024) and pen/strep (100 units/mL, Sigma P4333), and incubated at 37 °C with 5% CO_2. Cells were passaged every 2 days. For 3D array screening, 2×10^6 HeLa cells were incubated for 45 min

in 8 mL of serum free media with 25 μM of CellTracker^{TM} RED CMTPX (C34552, Life technologies). The labelled cells were spun down at 1000 g for 5 min, the supernatant discarded, and the cells were resuspended in 8 mL of DMEM with 10% FCS. 4 mL of this cell suspension was seeded onto a 3D single-network array and 3D double-network array placed into a 4 well chamber plate (1×10^6 cells/array), and additional 4 mL of media was added to each chamber well to insure all the hydrogel features were submerged. The arrays were incubated for 3 days (37 °C with 5% CO_2). The slides were washed with PBS, fixed with 4% formaldehyde in PBS for 10 min, and washed 3 times with PBS. The arrays were imaged with a Nikon Eclipse 50i microscope with the Pathfinder software (IMSTAR, France).

2.7. Statistical Analysis

Statistical analysis on the compression and tensile data sets was performed with InStat (GraphPad) software by comparing each column with all other columns (Bonferroni) using a one-way Anova.

3. Results and Discussion

3.1. Design and fabrication of 3D double-network hydrogel array

An overview of the methodology developed for the fabrication of the double-network 3D hydrogel arrays is shown in Fig. 1.

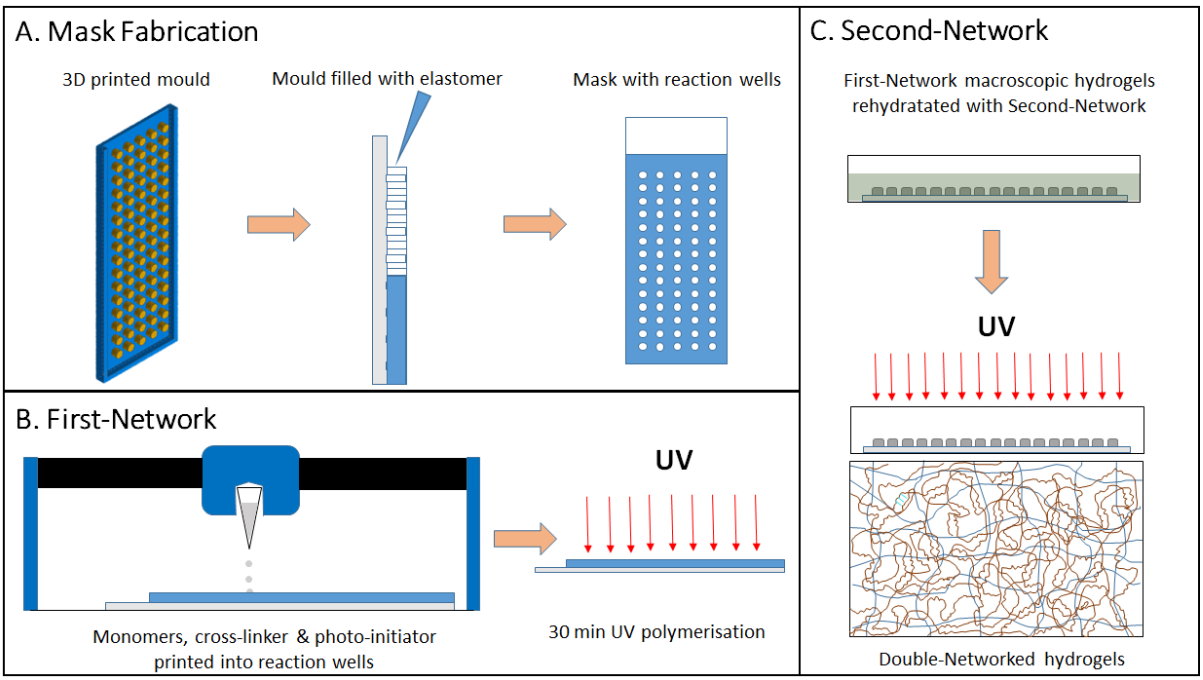

Fig. 1. An overview of the fabrication of the double-network 3D hydrogel arrays. (A) 3D moulds were printed using an Ultimaker 1 3D printer utilising a fused deposition modelling (FDM) strategy and PLA as the filament. The mould was attached to a glass microscope slide and filled with slow-curing silicone-based elastomer and allowed to solidify to produce a mask over a glass slide with 80 hollow cylinders (2.5 mm wide and 2 mm in height). (B) Into these cylinders ('reaction cells'), monomers, cross-linker and photo-initiator were printed to give a total volume of 3.9 µL/well. Hydrogels were generated by photo-polymerisation for 30 min under UV irradiation and the mask removed to leave 3D hydrogel features (thus generating the first-network). (C) Slides with the 3D hydrogels were submersed into a solution containing the components of the second network for 24 h. The excess of the second network components were removed by washing and the monomers were polymerised with UV light for 30 min.

A mould was designed (using Autodesk Inventor) to fit on a standard microscope glass slide (76 × 24 mm) and to consist of 80 cylindrical 'reaction wells' with an internal volume of 10 µL (2 mm high with a diameter of 2.5 mm) (Fig. 2A). The mould was made from polylactic acid (PLA) and printed using an Ultimaker 1 3D printer (see Table S1). The mould was fixed onto a glass slide and filled with a slow curing silicone-based elastomer (MoldStar). After 6 h curing, the mould and the glass slide were removed to leave a mask with the 80 cylindrical 'reaction wells' (Fig. 2B). This mask was then affixed to an agarose-coated glass slide. The mask was generated to fit the highest number of hydrogels allowing swelling of the features (for mask optimisation, see Fig. S1).

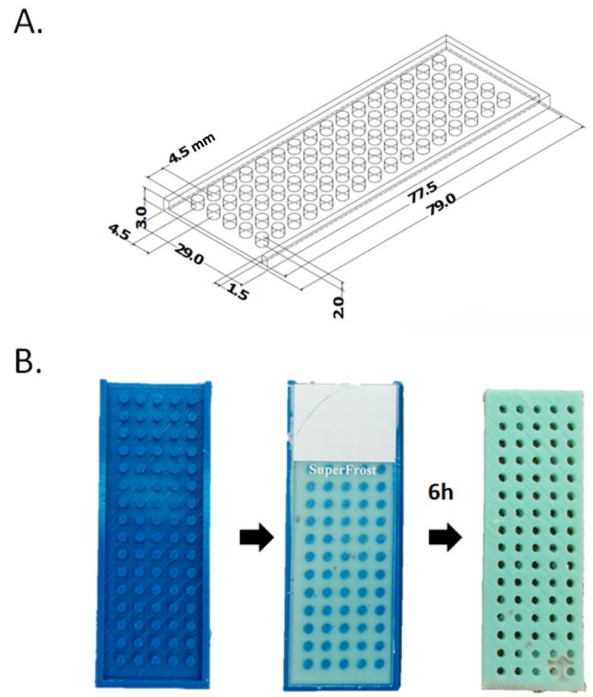

Fig. 2. (A) The 3D mould was designed using Autodesk Inventor and was composed of 16 rows of five cylinders (each 10 µL volume). The distance between columns and rows was 4.5 mm from center to center. (B) The mould was 3D printed using a customised Ultimaker 1 3D printer utilising the FDM strategy and 2.84 mm PLA as a filament. The mould was then affixed to a glass slide and the cavity was filled with a slow curing silicon-based elastomer (MoldStar) to produce a mask after 6 h of curing at room temperature. The mould and the slide were manually extracted to leave a mask with 80 'reaction wells'.

Into each of these wells, acrylate-based monomers were printed, altering their ratios and cross-linker *N,N'*-methylenebisacrylamide (MBA) levels along with 6 mol% of the photo-initiator 1-hydroxyclyclohexyl phenyl ketone (Table S2). The monomers chosen were 2-(acryloyloxyethyl) trimethylammonium chloride (AEtMA-Cl), *N,N*-diethylacrylamide (DEAA), *N*-isopropylacrylamide (NIPA), *N*-(1,1-dimethyl-3-oxobutyl)acrylamide (DMOBAA), 2-(dimethylamino)ethyl methacrylate (DMAEMA), poly(ethylene glycol) methacrylate (PEG_6MA), 2-carboxyethyl acrylate (CEA), ethylene glycol methacrylate phosphate (EMAP), and *N,N*-dimethylacrylamide (DMAA) (the monomer ratios used to produce the array are listed in Table S2). These monomer combinations have been shown to form shape stable hydrogels on a 2D polymer microarray that identified hydrogels supporting long-term human embryonic and mesenchymal stem cell culture [22,24]. All selected

monomers and photo-initiator solutions were prepared in NMP and the solutions dispensed in the reaction wells on the 80-well mask on agarose-coated slide using a bioprinter (PolyPico). Each of the 20 monomer combinations was dispensed into four different wells, into which cross-linker MBA was subsequently dispended to give final concentration of 8, 12, 16 and 20 %, ultimately generating 80 unique 1M solutions. The hydrogels were generated by *in situ* photo-polymerisation and the mask removed to give an array with 80 different 3D first network hydrogels (Fig. 3A).

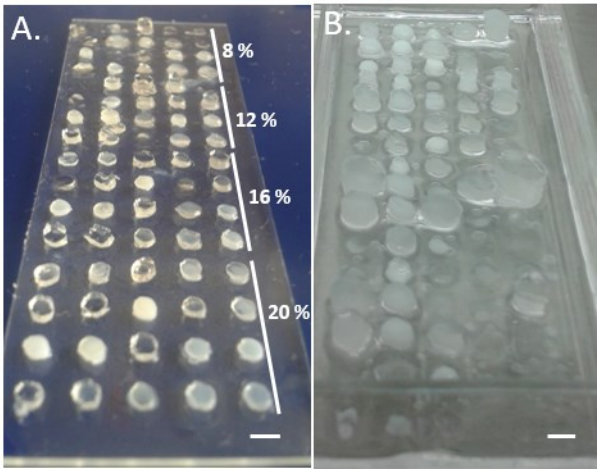

Fig. 3. (A) 3D single-network hydrogel array (not hydrated) with 20 different hydrogels at 8, 12, 16 and 20 mol% of MBA to give a total of 80 hydrogel features. (B) The corresponding 3D double-network hydrogel features after photo-polymerisation (and hydration) showing the swollen features (scale bar 2.5 mm). Note that the different hydrogels with the same cross-linker concentration show different swelling properties.

A variety of double-network systems have been developed [8,10]; however, the most suitable double-network for this array platform required a procedure whereby the first network absorbed the aqueous components of the second network prior to a second polymerisation step. The seminal work by Gong on double-networks used a first network composed of poly(2-acylamido-2-methylpropanesulfonic acid) (PAMPS) with a 4 mol% MBA as cross-linker and a loosely cross-linked (0.1 mol% MBA) polyacrylamide second-network [10], which resulted in hydrogels considerably stronger than the corresponding single component hydrogels. Here, the single-network arrays (polymerised at 1 M monomer concentration) were immersed in a 2M aqueous acrylamide solution with 0.1 mol% cross-linker (MBA) and

water soluble photo-initiator α-ketogluterate, with excess acrylamide removed prior to UV polymerisation. This gave a loosely cross-linked second polyacrylamide network in all the features, thus giving a 3D double-network hydrogel array (Fig. 3B). To examine the microstructures of the single- and double-network hydrogels, both types of arrays were fabricated, freeze dried, gold coated, and analysed by scanning electron microscopy (SEM) to reveal with distinct differences between the single- and double-network hydrogels (Fig. 4). Introduction of the polyacrylamide-based second-network resulted in highly 'porous' hydrogels (Fig. 4B, 4D, and 4F) compared to the corresponding single-network hydrogels consisting of same monomers and cross-linker ratio (Fig. 4A, 4C, and 4E).

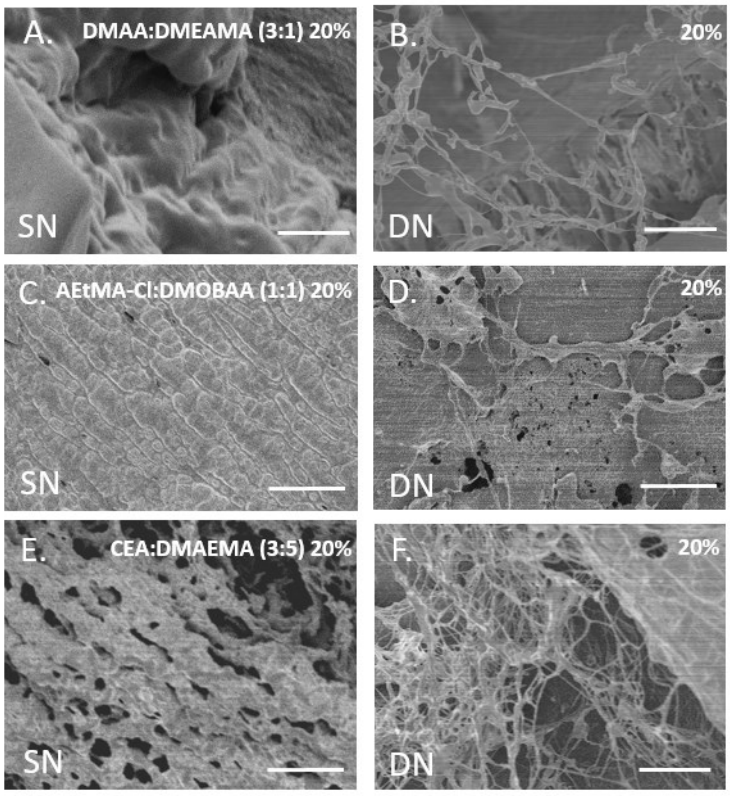

Fig. 4. Examples of SEM images of corresponding single- (SN) and double-network (DN) 'hydrogels' (scale bar 200 μm). All the hydrogels had 20 % MBA as a cross-linker for the first network and 0.1 % MBA the second-network. (A) Single-network DMAA:DMEAMA (polymerised in 3:1 monomer ratio, respectively) with 20 % of MBA. (B) Double-network DMAA:DMEAMA. (C) Single-network AEtMA-Cl:DMOBAA (polymerised in 1:1 monomer ratio) with 20 % of MBA. (D) Double-network AEtMA-Cl:DMOBAA. (E) Single-network CEA:DMAEMA (polymerised in 3:5 monomer ratio, respectively) with 20 % of MBA. (F) Double-network CEA:DMAEMA.

3.2. Mechanical properties of double-network hydrogels

To show that this array fabrication approach produces hydrogel features with varying mechanical properties, compressive stiffness and tensile strain testing was performed on 12 double-network hydrogels with the first networks including AEtMA-Cl:DEAA (1:1), DMOBAA:NIPA (7:1) and CEA:DMAEMA (3:5) at all four MBA concentrations (8, 12, 16, and 20 mol%). In addition, the corresponding single-network hydrogels were tested for comparison.

For compression testing (Fig. 5), two different strain rate conditions were examined, a low strain rate of 0.5 % min^{-1} and a high strain rate of 5 % min^{-1} [26,27]. The high strain rate was tested until 10 and 60 % strain, *i.e.,* until the reduction (%) in the initial sample height upon compression had been achieved. The rational for examining the hydrogels at different levels of strain was to obtain additional characterisation and understanding of the material properties, which allows a given material to be matched to a given function/purpose [25]. The single-network hydrogels made up of AEtMA-Cl:DEAA (1:1) at all MBA concentrations had insufficient mechanical strength to enable measurement; however, the corresponding double-network hydrogels showed relatively good compressive stiffness modulus (51–85 kPa) at the 0.5 % min^{-1} taken to 10 % strain (Fig. 5E). For example, with 16 % of MBA, AEtMA-Cl:DEAA exhibited a stiffness modulus (85 ± 7 kPa at 10 % strain) similar to that reported for cartilage (89.5 ± 48.6 kPa) [28]. At the higher compression rate (5 % min^{-1} taken to 10 %), the stiffness of double-networked AEtMA-Cl:DEAA increased with increasing amount of cross-linking in the first network. With CEA:DMAEMA (3:5), at 0.5 % min^{-1} compression rate, the stiffness of the double-network hydrogels increased with the amount of cross-linking (Fig. 5F, for the stress/strain curves see Fig. S2). At the highest compression rate of 5 % min^{-1} at 60 % strain, CEA:DMAEMA with 16 % MBA was the stiffest hydrogel (8.0 ± 2.4 MPa) in the series, and under which conditions all the corresponding single-network hydrogels disintegrated (Fig. 5D and 5F (iii)). Surprisingly, introduction of the second-network into DMOBAA:NIPA (7:1) did not result in improved compressive stiffness (Fig. 5G (iii)).

More detailed examination of hydrogel AEtMA-Cl:DEAA revealed that the compressive stiffness of these hydrogels was dependent on the molarity of the first-network with higher molarities producing stiffer hydrogels (Fig. S3A), whereas the ratio of the monomers did not have a notable effect (Fig. S3C). In addition, higher cross-linker concentration in the second network polyacrylamide resulted in increased stiffness (Fig. S3B).

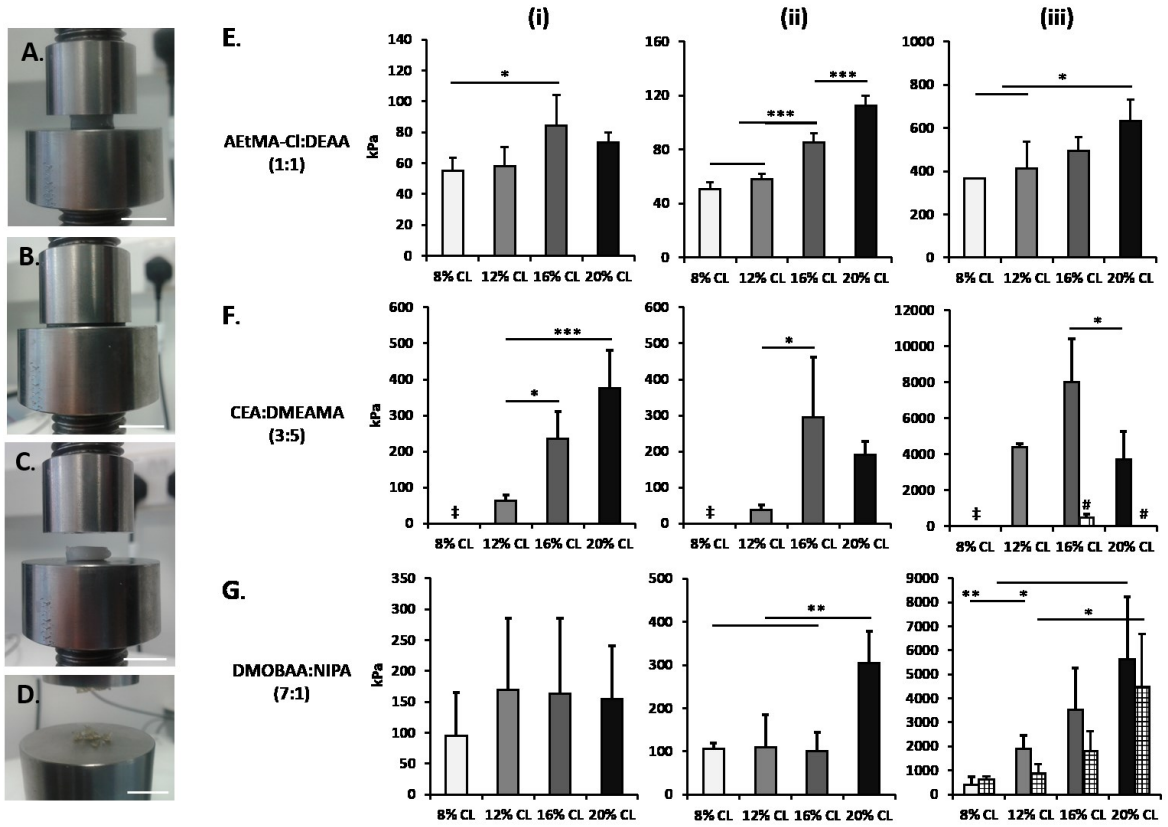

Fig. 5. Compression testing of representative hydrogels. Left: (A) Double-network (AEtMA-Cl:DEAA (1:1) 16 % MBA) in the INSTRON compression tester prior to sample compression (scale bar 10 mm); (B) At high compression; (C) After high compression, (D) Corresponding single-network hydrogel showing structural failure. Right: Compressive stiffness modulus (kPa) of the double-network hydrogels (E) AEtMA-Cl:DEAA (1:1), (F) CEA:DMAEMA (3:5) and (G) DMOBAA:NIPA (7:1) with 8, 12, 16 and 20 mol% of MBA, for both the double- (filled columns) and single-network hydrogels (hashed columns). (i) Slow compression (0.5 % of sample height per minute until 10 % of the sample is compressed); (ii) Fast compression (5 % of sample height per minute until 10 % of the sample is compressed); (iii) Fast compression to a high strain (5 % of the sample height per minute until 60% of the sample is compressed). # Denotes sample failure and ‡ the inability to form a solid hydrogel.

For tensile testing, single- and double-network hydrogels were prepared using a custom made ‘dog-bone’ shaped PDMS moulds (Fig. 6). Extension was performed at a rate of 30 % min^{-1} of the sample length until failure. Again, the single-network AEtMA-Cl:DEAA (1:1) hydrogels did not have sufficient mechanical properties to be tested, which were significantly improved by the introduction of the second-network (Fig. 7B and 7C), with the hydrogel with 16 % of MBA in the first network giving the highest extension prior to failure (520 % failure

strain, ~6 times its original length). Conversely, with DMOBAA:NIPA (7:1), the addition of the second network did not result in better extension properties (Fig 7D). CEA:DMAEMA (3:5), which had the best compressive properties, demonstrated overall relatively poor strain (Fig. 7E). The failure strain was dependent on the molarity of the networks with only 1M first network and 2M second network (0.1 % cross-linking) combination producing extendable hydrogels with AEtMA-Cl:DEAA (Fig. S3D and S3E), with DEAA the monomer primarily responsible for the high extension properties of these hydrogels (Fig. S3F).

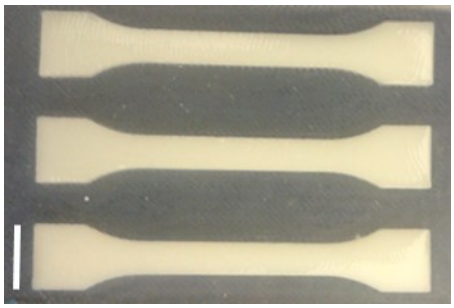

Fig. 6. To prepare hydrogel samples for tensile testing, PDMS 'dog-bone' moulds (890 µL volume) were used (scale bar 10 mm). The moulds were filled with the first network components, photo-polymerised, and then submersed in a solution containing the second network components and photo-polymerised again to create the double-network hydrogels.

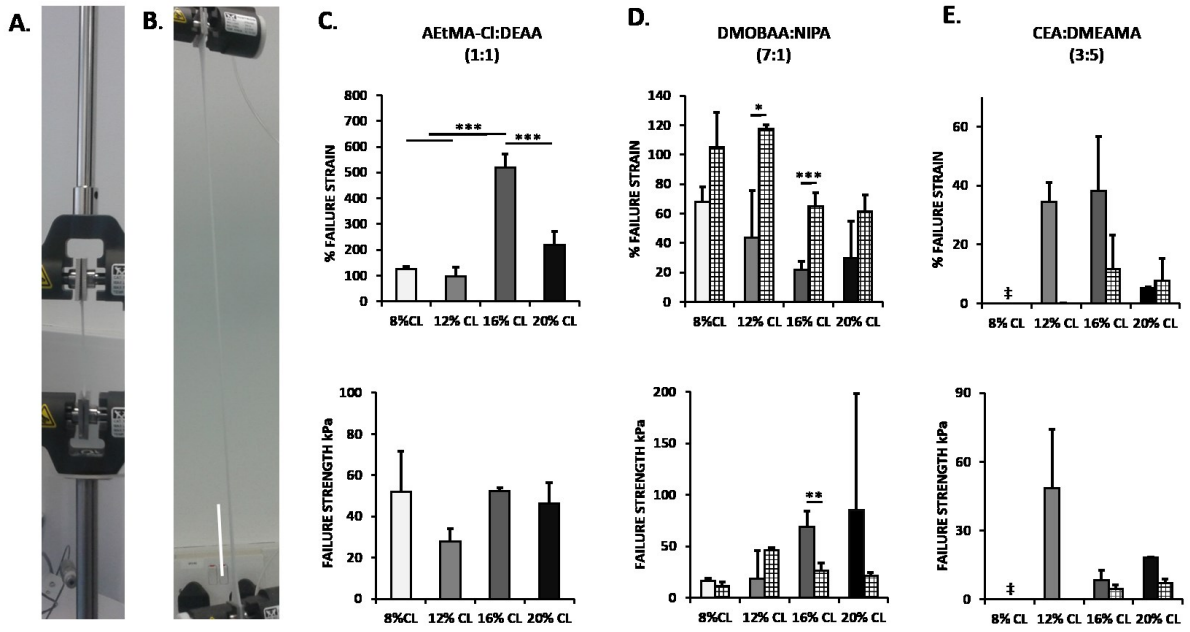

Fig. 7. Failure strain (%) and failure strength (kPa) of double-network hydrogels (filled columns) and single-network hydrogels (hashed columns). (A) Double-network hydrogel

AEtMA:Cl:DEAA (1:1) with 16% MBA in the INSTRON tensile testing instrument; (B) extended until failure (scale bar 100 mm). Failure strain (%) (top graphs) and % failure strength (kPa) (bottom graphs) of (C) AEtMA-Cl:DEAA (1:1), (D) DMOBAA:NIPA (7:1) and (E) CEA:DMAEMA (3:5) single-network hydrogels at 16 and 20 mol% MBA and the corresponding double-network hydrogels at 12, 16 and 20 mol% MBA. AEtMA-Cl:DEAA (1:1) single-network hydrogels had insufficient strength for mechanical testing. DMOBAAA:NIPA (7:1) single-network hydrogels could be tested at all four MBA concentrations, while the CEA:DMAEMA (3:5) could only be tested at 16 and 20 % MBA concentration. ‡ Denotes the inability to form a solid hydrogel.

3.3. Cell-based screening on 3D hydrogel arrays

To determine whether these 3D hydrogel arrays are suitable for cell-based screening, HeLa cells were seeded onto both single- and double-network 3D hydrogel arrays and incubated for 3 days, after which selected features were imaged and the cell binding assessed. The single- and double-network arrays both withstood prolonged incubation in biological media. Binding of the cells was observed on features in both the single- and double-network arrays demonstrating that inclusion of the second-network did not prevent cellular attachment (Fig. 8). In particular, double-network hydrogel AEtMA-Cl:DMOBAA (5:3 monomer ratio, respectively, with 20 % MBA) showed good cell binding with cells largely covering the surface (Fig. 8H) demonstrating the utility of this array platform for the generation of wide range of biocompatible features. However, no infiltration of cells into the hydrogels was observed possibly due to the high cross-linker concentration used in these hydrogels.

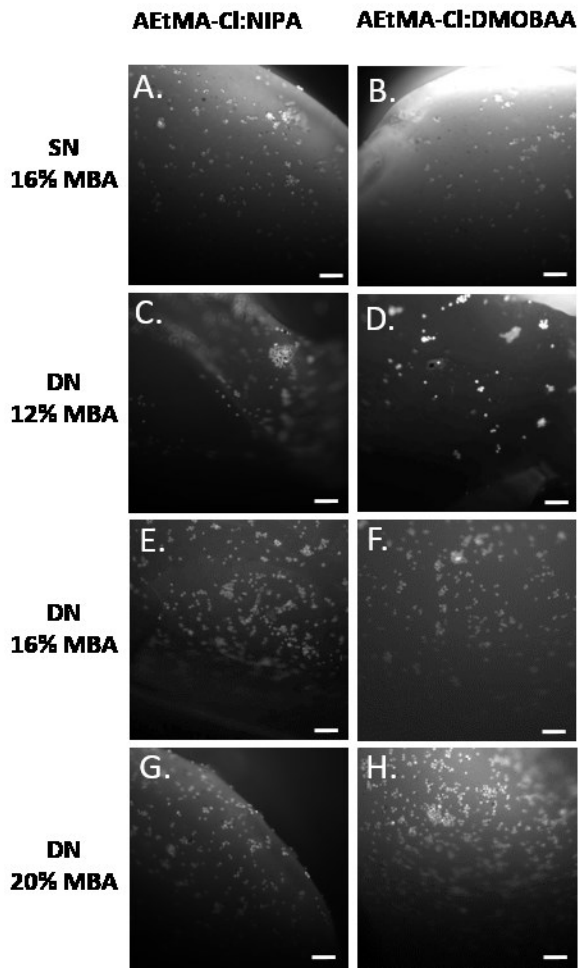

Fig. 8. Semi-confocal images of hydrogel features on 3D arrays after incubation with HeLa cells (scale bar 100 μm). HeLa cells were stained with Cell Tracker Red (25 μM in DMEM) and seeded onto a single and double-network 3D hydrogel array (1×10^6 cells/array) and cultured for 3 days. Cells were fixed with 4 % paraformaldehyde and images were captured with a Nikon eclipse 50i microscope (×10, $\lambda_{Ex/Em}$ 577/607 nm) and analysed with Pathfinder software (IMSTAR). (A and B) HeLa cells growing on the surface of the single-network hydrogels AEtMA-Cl:NIPA (3:1) and AEtMA-CL:DMOBAA (5:3) at 16 % MBA. (C–H) HeLa cells growing on the surfaces of the 3D double-network hydrogels of AEtMA-Cl:NIPA (3:1) and AEtMA-Cl:DMOBAA (5:3) at 12, 16 and 20 % MBA.

4. Conclusions

A new 3D array platform that allows the fabrication of up to 80 macroscopic single- and double-network hydrogels was developed. A 3D mould for the array was designed, printed and subsequently used to generate a mask that was placed on a glass slide to produce 80 ‘reaction wells’. Into these wells acrylate-based monomers were printed to generate single-network hydrogels on a microscope slide that was subsequently submersed in the components

of the second-network and photo-polymerised to generate the 3D double-network array. Mechanical testing revealed that this 3D double-network array platform allows the production of hydrogels with a wide range of tensile and compressive properties. The suitability of the 3D hydrogel array for cell-based studies was assessed with HeLa cells showing that the features withstood incubation in biological media and could be imaged and assessed using a high-throughput platform. This platform can be adapted to different hydrogels by altering the monomers used and the second network for a given array can be readily altered, providing the flexibility to generate wide variety of double-network hydrogels with unique properties. In addition, the mask can be customised to alter the number and dimensions of the features. This 3D hydrogel array platform therefore represents a useful new tool in material and biomaterial discovery.

Disclosures

The authors report no conflict of interest.

Acknowledgments

We thank the ERC (ERC-2013-ADG 340469 ADREEM) for funding, Dr Logan MacKay for helpful discussions on 3D printing, and PolyPico (Ireland) for their technical support and helpful advice.

Appendix A. Supplementary data

References

[1] B.K. Mann, J.L. West, Cell adhesion peptides alter smooth muscle cell adhesion, proliferation, migration, and matrix protein synthesis on modified surfaces and in polymer scaffolds, J. Biomed. Mater. Res. 60 (2002) 86–93.

[2] E.S. Place, N.D. Evans, M.M. Stevens, Complexity in biomaterials for tissue engineering, Nat. Mater. 8 (2009) 457–470.

[3] P.M. Gilbert, K.L. Havenstrite, K.E.G. Magnusson, A. Sacco, N.A. Leonardi, P. Kraft,

et al., Substrate elasticity regulates skeletal muscle stem cell self-renewal in culture, Science. 329 (2010) 1078–1081.

[4] N. Huebsch, P.R. Arany, A.S. Mao, D. Shvartsman, O.A. Ali, S.A. Bencherif, et al., Harnessing traction-mediated manipulation of the cell/matrix interface to control stem-cell fate, Nat. Mater. 9 (2010) 518–526.

[5] C. Yang, M.W. Tibbitt, L. Basta, K.S. Anseth, Mechanical memory and dosing influence stem cell fate, Nat. Mater. 13 (2014) 645–652.

[6] A.J. Engler, S. Sen, H.L. Sweeney, D.E. Discher, Matrix Elasticity Directs Stem Cell Lineage Specification, Cell. 126 (2006) 677–689.

[7] M.A. Haque, T. Kurokawa, J.P. Gong, Super tough double network hydrogels and their application as biomaterials, Polymer. 53 (2012) 1805–1822.

[8] J.Y. Sun, X. Zhao, W.R.K. Illeperuma, O. Chaudhuri, K.H. Oh, D.J. Mooney, et al., Highly stretchable and tough hydrogels, Nature. 489 (2012) 133–136.

[9] S. Ronken, D. Wirz, A.U. Daniels, T. Kurokawa, J.P. Gong, M.P. Arnold, Double-network acrylamide hydrogel compositions adapted to achieve cartilage-like dynamic stiffness, Biomech. Model. Mechanobiol. 12 (2013) 243–248.

[10] J.P. Gong, Y. Katsuyama, T. Kurokawa, and Y. Osada, Double-Network Hydrogels with Extremely High Mechanical Strength, Adv. Mater. 15 (2003) 1155–1158.

[11] D. Myung, W. Koh, J. Ko, Y. Hu, M. Carrasco, J. Noolandi, et al., Biomimetic strain hardening in interpenetrating polymer network hydrogels, Polymer. 48 (2007) 5376–5387.

[12] D.G. Anderson, S. Levenberg, R. Langer, Nanoliter-scale synthesis of arrayed biomaterials and application to human embryonic stem cells, Nat. Biotechnol. 22 (2004) 863–866.

[13] Hitoshi, Mizomoto, The synthesis and screening of polymer libraries using a high throughput approach, University of Southampton, 2004.

[14] R.S. Tare, F. Khan, G. Tourniaire, S.M. Morgan, M. Bradley, R.O.C. Oreffo, A microarray approach to the identification of polyurethanes for the isolation of human skeletal progenitor cells and augmentation of skeletal cell growth, Biomaterials. 30 (2009) 1045–1055.

[15] D.C. Hay, S. Pernagallo, J.J. Diaz-Mochon, C.N. Medine, S. Greenhough, Z. Hannoun, et al., Unbiased screening of polymer libraries to define novel substrates for functional hepatocytes with inducible drug metabolism, Stem Cell Res. 6 (2011) 92–102.

[16] A. Hansen, L. McMillan, A. Morrison, J. Petrik, M. Bradley, Polymers for the rapid and effective activation and aggregation of platelets, Biomaterials. 32 (2011) 7034–7041.

[17] M. Wu, H. Bridle, M. Bradley, Targeting Cryptosporidium parvum capture, Water Res. 46 (2012) 1715–1722.

[18] S. Venkateswaran, M. Wu, P.J. Gwynne, A. Hardman, A. Lilienkampf, S. Pernagallo, et al., Bacteria repelling poly(methylmethacrylate-co-dimethylacrylamide) coatings for biomedical devices, J. Mater. Chem. B. 2 (2014) 6723–6729.

[19] S. Pernagallo, M. Wu, M.P. Gallagher, M. Bradley, Colonising new frontiers—microarrays reveal biofilm modulating polymers, J. Mater. Chem. 21 (2011) 96–101.

[20] A.L. Hook, C.Y. Chang, J. Yang, J. Luckett, A. Cockayne, S. Atkinson, et al., Combinatorial discovery of polymers resistant to bacterial attachment, Nat. Biotechnol. 30 (2012) 868–875.

[21] A. Hansen, H.K. Mjoseng, R. Zhang, M. Kalloudis, V. Koutsos, P.A de Sousa, and M. Bradley, High-Density Polymer Microarrays: Identifying Synthetic Polymers that Control Human Embryonic Stem Cell Growth, Adv. Healthc. Mater. 3 (2014) 848–853.

[22] R. Zhang, H.K. Mjoseng, M.A. Hoeve, N.G. Bauer, S. Pells, R. Besseling, et al., A thermoresponsive and chemically defined hydrogel for long-term culture of human embryonic stem cells, Nat. Commun. 4 (2013) 1335–1342.

[23] C. Mangani, A. Lilienkampf, M. Roy, P.A. de Sousa, M. Bradley, Thermoresponsive hydrogel maintains the mouse embryonic stem cell “naïve” pluripotency phenotype, Biomater. Sci. (2015) 1371–1375.

[24] C.R.E. Duffy, R. Zhang, S.E. How, A. Lilienkampf, P.A. De Sousa, M. Bradley, Long term mesenchymal stem cell culture on a defined synthetic substrate with enzyme free passaging, Biomaterials. 35 (2014) 5998–6005.

[25] A. Callanan, N.F. Davis, T.M. McGloughlin, M.T. Walsh, The effects of stent interaction on porcine urinary bladder matrix employed as stent-graft materials, J. Biomech. 47 (2014) 1885–1893.

[26] J.A. Steele, S.D. McCullen, A. Callanan, H. Autefage, M.A. Accardi, D. Dini, et al., Combinatorial scaffold morphologies for zonal articular cartilage engineering, Acta Biomater. 10 (2014) 2065–2075.

[27] M.A. Accardi, S.D. McCullen, A. Callanan, S. Chung, P.M. Cann, M.M. Stevens, et al., Effects of Fiber Orientation on the Frictional Properties and Damage of Regenerative Articular Cartilage Surfaces, Tissue Eng. Part A. 19 (2013) 2300–2310.

[28] S.D. McCullen, H. Autefage, A. Callanan, E. Gentleman, M.M. Stevens, Anisotropic Fibrous Scaffolds for Articular Cartilage Regeneration, Tissue Eng. Part A. 18 (2012) 2073–2083.